THE ASTROPHYSICAL JOURNAL, 360:685–695, 1990 September 10

COBE DIFFERENTIAL MICROWAVE RADIOMETERS: INSTRUMENT DESIGN AND IMPLEMENTATION

G. SMOOT,[1] C. BENNETT,[2] R. WEBER,[3] J. MARUSCHAK,[3] R. RATLIFF,[3] M. JANSSEN,[4] J. CHITWOOD,[3] L. HILLIARD,[3] M. LECHA,[3] R. MILLS,[3] R. PATSCHKE,[3] C. RICHARDS,[3] C. BACKUS,[5] J. MATHER,[2] M. HAUSER,[2] R. WEISS,[6] D. WILKINSON,[7] S. GULKIS,[4] N. BOGGESS,[2] E. CHENG,[2] T. KELSALL,[2] P. LUBIN,[8] S. MEYER,[6] H. MOSELEY,[2] T. MURDOCK,[9] R. SHAFER,[2] R. SILVERBERG,[2] AND E. WRIGHT[10]

Received 1989 December 8; accepted 1990 March 12

ABSTRACT

Differential Microwave Radiometers (DMRs) at frequencies of 31.5, 53, and 90 GHz (9.5, 5.7, and 3.3 mm) have been designed and built to map the large angular scale variations in the brightness temperature of the cosmic microwave background radiation. The instrument is being flown aboard NASA's *Cosmic Background Explorer* (*COBE*) satellite, launched 1989 November 18. Each receiver input is switched between two antennas pointing 60° apart on the sky. The satellite spins at 0.8 revolutions per minute to interchange the antenna directions every half-rotation. The satellite is in near-polar orbit with the orbital plane precessing at 1° per day, causing the beams to scan the entire sky in 6 months. In 1 year of observation, the instruments are capable of mapping the sky to an rms sensitivity of 0.1 mK per 7° field of view. This translates to a per pixel sensitivity of $\Delta T/T_{\rm CMB} = 4 \times 10^{-5}$ (1 σ) and a dipole sensitivity of 5×10^{-6} (1 σ) in 1 year. The mission and the instrument have been carefully designed to minimize the need for systematic corrections to the data.

Subject headings: cosmic background radiation — instruments

I. INTRODUCTION

The cosmic microwave background (CMB) radiation, first detected by Penzias and Wilson (1965), is thought to be a remnant from a hot dense phase of the early universe (Gamov 1948*a*, *b*; Alpher and Herman 1948, 1949, 1950, 1975; Dicke *et al.* 1965). We have developed and tested three Differential Microwave Radiometers (DMRs) for the *Cosmic Background Explorer* (*COBE*)[11] satellite to detect and map the anisotropy of the CMB on large angular scales. These radiometers represent a realization of space-qualified, room temperature, and passively cooled differential radiometers of high sensitivity, high stability, and immunity to external effects.

Cosmologically interesting anisotropies would be expected from effects such as an asymmetric expansion of the universe (Thorne 1967; Hawking 1969), large-scale irregularities in the distribution of matter or energy, as are needed for the formation of galaxies and clusters of galaxies (Sachs and Wolfe 1967), rotation of the universe (Collins and Hawking 1973; Hawking 1969; Gödel 1949; Batakis and Cohen 1975), gravity wave radiation (Burke 1975; Grishchuk and Zel'dovich 1978), cosmic strings (Vilenkin 1985), or other dynamic effects important in the evolution of the universe. Predictions for the magnitudes of such anisotropies depend upon assumptions about the large-scale structure and content of the universe. Hence, measuring or setting limits upon such anisotropies is a powerful constraint on cosmological models. Efforts have been made to detect large angular scale anisotropies from experiments performed on the ground, from aircraft, and from balloons (Boughn *et al.* 1990; Lubin *et al.* 1985; Fixsen, Cheng, and Wilkinson 1983; Cheng *et al.* 1979), as well as from a Soviet spacecraft (Strukov and Skulachev 1984, 1988; Strukov *et al.* 1988; Klypin *et al.* 1987). Current upper limits on a quadrupole anisotropy are $\Delta T/T_{\rm CMB} \sim 7 \times 10^{-5}$. The only confirmed CMB anisotropy detected on any angular scale is a dipole anisotropy. The amplitude of the dipole anisotropy in the CMB, detected at the 3 mK level ($\Delta T/T_{\rm CMB} \sim 10^{-3}$ with $T_{\rm CMB} \sim 3$ K currently), is thought to result from the Doppler shift of the motion of the solar system with respect to the CMB (Smoot, Gorenstein, and Muller 1977; Cheng *et al.* 1979; reviewed by Wilkinson 1986, 1987 and Partridge 1987). In addition, the motion of the Earth around the Sun is observed to modulate this anisotropy at the level of 0.3 mK. The achievable sensitivity of CMB anisotropy measurements from above the Earth's atmosphere is limited ultimately by competing emission from local astronomical sources.

The Differential Microwave Radiometer (DMR) experiment was designed to obtain definitive measurements of the anisotropy of the CMB. In particular, the experimental goal is to measure the brightness variation of the CMB over the entire sky with an accuracy which is limited primarily by our ability to account for the local astronomical emission. Measurements were originally planned at four frequencies to allow the separation of local emission from the CMB. After a reassessment of the galactic emission in 1984, the original low-frequency 23 GHz channel was replaced by a series of balloon flights with a 19 GHz maser receiver system (Boughn *et al.* 1990), and the 53 and 90 GHz radiometers were redesigned to be passively

[1] University of California, Berkeley.
[2] Laboratory for Astronomy and Solar Physics, NASA/Goddard Space Flight Center.
[3] Instrument Division, NASA/Goddard Space Flight Center.
[4] NASA Jet Propulsion Laboratory.
[5] STX Corporation.
[6] Massachusetts Institute of Technology.
[7] Princeton University.
[8] University of California, Santa Barbara.
[9] General Research Corporation.
[10] University of California, Los Angeles.
[11] The National Aeronautics and Space Administration/Goddard Space Flight Center (NASA/GSFC) is responsible for the design, development, and operation of the *Cosmic Background Explorer*, under the guidance of the *COBE* Science Working Group. GSFC is also responsible for the software development through to the final processing of the space data.

cooled to 140 K to improve their sensitivity. With these changes, we estimated a sensitivity of at least 0.1 mK per field of view for the 53 and 90 GHz frequency channels and 0.25 mK for the 31.5 GHz radiometer could be achieved with a mission lifetime of at least 1 year. To achieve such sensitivity, the measurement technique is designed to be differential on several time scales. Severe requirements are placed on the stability of the instrument and its immunity to systematic effects so that these do not become limiting factors in the CMB measurements. If the experiment works properly, we estimate that the data obtained at 19.0, 31.5, 53, and 90 GHz, and the data from the other *COBE* instruments, will allow us to model the astrophysical foregrounds, which are currently not well determined at these frequencies. We will thus separate the galactic and cosmic background signals at a level comparable to the instrument sensitivity.

Long flight duration, total sky coverage, and elimination of atmospheric background make a satellite a particularly attractive platform from which to measure the CMB anisotropy. The DMR experiment is one of three complementary experiments to be flown on the *Cosmic Background Explorer* (*COBE*) mission (Mather 1982; Mather and Kelsall 1980), which was proposed to NASA in 1974. Figure 1 shows a line drawing of the *COBE* spacecraft. The DMR experiment is located around the periphery of a central superfluid helium cryostat which contains two infrared experiments. These experiments are a spectrometer (FIRAS, the Far-Infrared Absolute Spectrophotometer) to measure the sky spectrum from $\lambda = 100$ μm to 1 cm, including the CMB radiation, and an absolute infrared radiometer (DIRBE, the Diffuse Infrared Background Experiment) which maps the sky from $\lambda = 1$–300 μm and looks for the cumulative emission from primeval galaxies and other luminous early objects. The instruments are mounted inside a fixed Earth/Sun shield, seen in Figure 1, which provides a stable thermal environment. The shield is made of 12 honeycomb panels covered with multilayer insulating blankets, alternating with blanketed segments with no rigid panels.

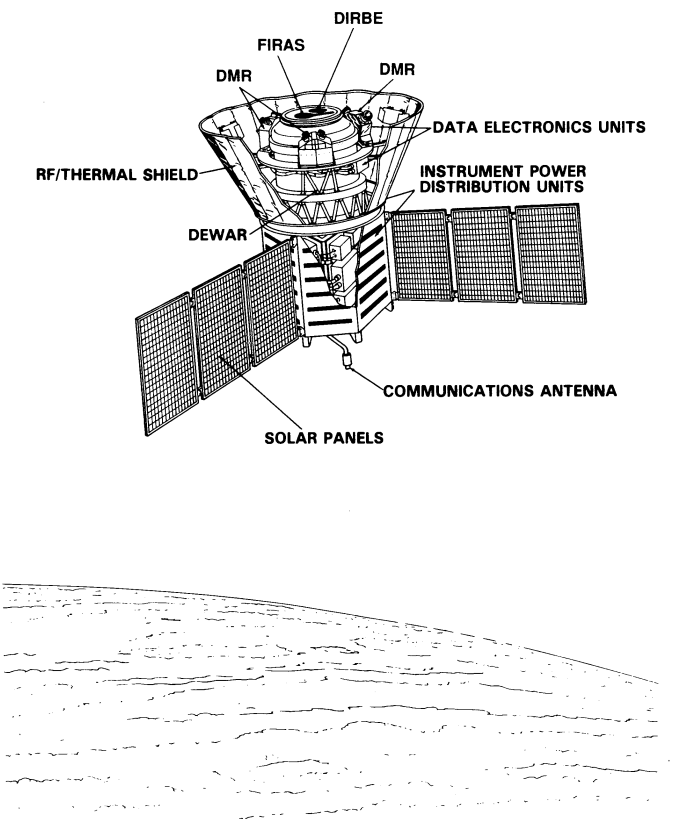

FIG. 1.—The *Cosmic Background Explorer* (*COBE*) satellite showing the Differential Microwave Radiometers (DMRs), Data Electronics Units (DEUs), and Instrument Power Distribution Units (IPDUs) as mounted on the *COBE* spacecraft. The spacecraft spins about its axis of symmetry.

The *COBE* satellite was launched on a Delta rocket on 1989 November 18 into a 900 km altitude terminator orbit inclined at 99°. The quadrupole moment of the Earth precesses the orbit 1° per day; the ascending node of the orbital plane thus follows the terminator, making the orbit Sun-synchronous. The orbit is very similar to the *IRAS* orbit, except that *COBE* has a 6 pm ascending node while *IRAS* had a 6 am ascending node. The satellite rotates at 0.8 revolutions per minute around its axis of symmetry, enabling scanning by instruments pointed off axis (DIRBE and DMR), while the near-polar orbit and its precession allow full sky coverage to be obtained in 6 months.

The satellite spin axis is pointed 94° from the Sun and generally away from the Earth. The spin angular momentum of the spacecraft is cancelled by two large internal momentum wheels. The zero net spin angular momentum system allows the spin axis to be smoothly rotated 360° around the solar direction once per orbit. The average angle between the orbital velocity vector and the spin axis is 96°, which means that the wind from any residual atmosphere at 900 km altitude does not directly impact the instruments inside the Earth/Sun shield. The attitude of the spacecraft is controlled in three axes by reaction wheels and determined by Sun sensors, Earth sensors, and gyroscopes. Electromagnets ("torquer bars") unload reaction wheel momentum by applying torque against the Earth's magnetic field. The *COBE* attitude control system is described in detail by Bromberg and Croft (1985).

The remainder of this paper will discuss the design criteria of the DMR experiment, the instrument hardware and testing, and the important radiometer characteristics. The ground calibration will be discussed in a future paper.

II. DESIGN CONSIDERATIONS FOR THE DMR EXPERIMENT

There are two crucial aspects in making an anisotropy measurement. One is to design the experiment to minimize or cancel systematic errors and to reveal any significant unsuspected effects, and the second is to distinguish among the various cosmic sources of anisotropies.

Two strategies are used to reveal instrumentally induced systematic errors. The first involves performing special tests to check each effect of concern. For example, immersing the instrument in a controlled external magnetic field tests the magnetic susceptibility, and deliberately varying power supply voltages tests the instrument immunity to supply variations. The second strategy involves chopping of the source signal to eliminate intrinsic instrumental asymmetries. For example, switching the radiometer input between two antennas and rotating the entire instrument help eliminate such potential systematic errors.

Sections II*a*–II*d* below discuss possible instrumentally induced systematic errors, while §§ II*e* and II*f* discuss the cosmic sources which the experiment must be capable of rejecting or distinguishing from the CMB anisotropies.

a) Instabilities and Asymmetries: Need for a Differential Radiometer

A differential radiometer is a device whose output voltage is proportional to the difference in power received by two horn

antennas (see, for example, Evans and McLeish 1977). The voltage is calibrated in units of antenna temperature (a linear measure of RF power) by measuring the voltage change for a known change in temperature of a source filling the beam of one antenna.

The use of a differential radiometer obviates the need for making absolute measurements with accuracy at the 10^{-4} level. This reduces the need for gain stability by the ratio of the effective system noise temperature plus signal to that of the radiometer imbalance (a factor of a few thousand). Rotating the radiometer (in this case, by rotating the entire *COBE* spacecraft) modulates the anisotropy in the background radiation to distinguish it from asymmetry in the apparatus. True anisotropies will yield a difference signal which changes sign when the sky patches observed by each beam are interchanged; an instrumental asymmetry or offset remains constant to the extent that the apparatus itself is unaffected by rotation. Signals which arise from asymmetries in the instrument will be reduced further by the orbital and precessional switching. The limitation of this approach is that the radiometer detects only the difference in sky temperatures and not the absolute intensity. Substantial data processing is required to convert differential measurements between all observed pixel pairs into sky maps. The resulting maps have an arbitrary overall zero level in the temperature scale.

b) Thermal Stability

The instrument must give stable and reliable results, implying that it be kept and operated in a benign environment. Specifically, the instrument must be well regulated thermally; typically temperatures should be stable to 0°.1 C for periods of hours. In addition to the thermal stability, each radiometer must be as nearly thermally symmetric as possible to minimize the effects which differential thermal changes would have on the differential temperature measurement. Great care must be taken to keep each horns of a pair at the same temperature.

The Earth/Sun shield provides a stable thermal environment for the radiometers. The inner surface of the shield must have a temperature of less than 240 K and an infrared emissivity of about 0.04 to assure that the radiometers can be controlled at their required operating temperatures. This requirement is easily met.

c) Radio Frequency Interference

A satellite at *COBE*'s 900 km orbit can be exposed to radio frequency interference (RFI) of terrestrial origin at levels as high as 10 V m^{-1}. Several steps were taken to minimize the instrument's susceptibility to RFI. First, the Earth/Sun shield also serves as a RFI shield. The shield must be RF-tight, with the requirement that 2 GHz signals from the surface of the Earth reach the instrument apertures at levels limited by diffraction over the top edge of the shield rather than transmission through the shield. Second, all the electronics and microwave circuits are in shielded boxes. Third, all harnesses are carefully grounded with RF shielding on cable connectors and penetrations. Fourth, power supply leads within the radiometer boxes use ferrite feedthrough filters where appropriate. In addition, there are natural protections against RFI. For example, RFI with wavelengths longer than waveguide cutoff will be strongly attenuated at the receiver front end. The high degree of redundancy of measurements as well as the many modulation rates in the experiment will help us to discriminate against occasional Earth-fixed sources.

d) Magnetic Susceptibility

Magnetic fields are expected from the *COBE* spacecraft torquer bars and from the Earth. The concern is that magnetic fields can affect the operation of ferrite components, in particular, the ferrite switches which perform differencing between the two antennas (see § III*b* below). Such magnetic effects are of even greater concern if the magnetic fields are modulated at the spacecraft spin rate, which is the case for the Earth's field and the spacecraft torquer bar fields.

Magnetic shielding was employed to reduce the susceptibility of the instrument to external magnetic fields. The requirement was to achieve a magnetic susceptibility below 0.2 mK G^{-1} to reduce the magnetic effects to be removed in ground data processing.

e) Galactic Emission: Choice of Measurement Frequency

The instrument sensitivity required depends on the choice of frequency because the expected levels of the signal and the competing foregrounds are both frequency dependent.

The largest astrophysical impediment to the measurement of the large-scale anisotropy of the cosmic background radiation is diffuse galactic radiation. Preferably, anisotropy measurements should be done at a frequency where the galactic contribution is minimized. Estimates of the galactic contribution to a 7° full width at half-maximum (FWHM) beam on the galactic plane are identified in Figure 2. Synchrotron radiation from high-energy electrons in the galactic magnetic field and thermal bremsstrahlung from ionized hydrogen H II regions are the dominant sources of emission at centimeter wavelengths. At far-infrared wavelengths, thermal emission from interstellar dust predominates. Since galactic radiation is significant, its angular distribution must be well understood before attributing anisotropy to the CMB. The CMB aniso-

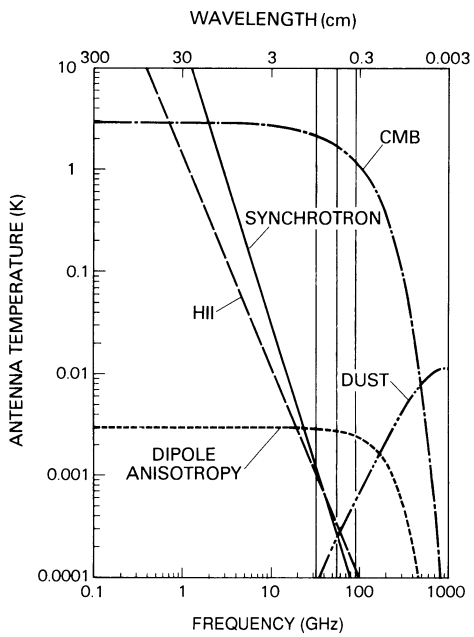

FIG. 2.—Spectra of the important sources of astronomical emission in the galactic plane which "interfere" with measurements of the cosmic microwave background radiation. The synchrotron and H II emission from our galaxy dominate at the lower frequencies (i.e., at 31 GHz), while interstellar dust emission begins to dominate at the higher frequencies (i.e., at 90 GHz). The three vertical lines indicate the three DMR frequencies at 31.5, 53, and 90 GHz. The CMB curves assume a Planckian spectrum.

tropy and galactic contributions all have different frequency spectra, so comparison of measurements at different frequencies can be used to identify the various contributions. This procedure is, of course, limited by the accuracy to which the spectra are known. Figure 2 indicates a window in the region 50–100 GHz where the total galactic emission is low. Exactly where this minimum occurs depends on how the dust emission is distributed spatially and spectrally. Within this window, the bands between 51.4 and 54.25 GHz and between 86 and 92 GHz are protected for radio astronomy; thus, frequencies of 53 and 90 GHz were selected for this experiment. A radiometer at 31.5 GHz frequency is also included because it is partially protected for radio astronomy (31.3–31.8 GHz), and because both good CMB data and useful galactic emission data can be obtained at that frequency. Galactic synchrotron emission gives rise to a signal which goes approximately as $T_{syn} \sim 1.5 f_{GHz}^{-2.8}$ K, while emission from H II regions in the plane of the galaxy gives $T_{H\,II} \sim 0.4 f_{GHz}^{-2.1}$ K. The results from the 19 GHz balloon flights of Boughn *et al.* (1990), mentioned earlier, and the DMR 31.5 GHz radiometer will be particularly valuable in modeling the galactic H II and synchrotron emissions so as to distinguish them from the CMB signal.

f) *Sun, Earth, and Moon Immunity: Earth/Sun Shield and Low Sidelobe Antennas*

We require that the microwave signal level from the Earth entering the radiometers be reduced to less than 0.1 mK at all times. The data from times where the diffracted Earth radiation is significant must either have a correction applied or be ignored. The Sun, which is always at the same angle to the spacecraft, must contribute less than 0.001 mK to avoid the application of data corrections. As discussed earlier, the radiometers are mounted inside a fixed Earth/Sun shield which protects them from direct illumination from the Sun, Earth, and terrestrial radio frequency interference. The radiometers never view the Sun, and only during summer solstice does the limb of the Earth appear occasionally above the shield edge. Extremely low sidelobe antennas, with better than 75 dB rejection at 90° off-axis and the Earth/Sun shield, are required to meet the required reductions of the microwave radiation levels from the Earth and Sun.

When the Moon is in the beam, the data cannot be used in the generation of sky maps. However, the Moon will serve as an external calibrator with an on-axis signal strength of as much ≈ 1 K, depending on the phase angle of the Moon.

III. INSTRUMENT DESCRIPTION

a) *Configuration*

The entire instrument consists of three radiometers and an electronics subsystem (Fig. 3). Each of these subsystems is fully redundant to assure system reliability. Thus, in the electronics subsystem, there are two digital electronics units (DEUs), each of which controls one of two channels (A and B) of each of the three radiometers. These DEUs provide timing and control signals, and digitize the analog radiometer and engineering signals from their respective channels. Instrument power distribution units (IPDUs) provide conditioned power to all units and handle power related signals. The DEUs and IPDUs provide all necessary communication with the spacecraft telemetry system. Physically, the system is contained in seven separate units which are located on the spacecraft as shown in Figure 1. The three differential microwave radiometer "heads"

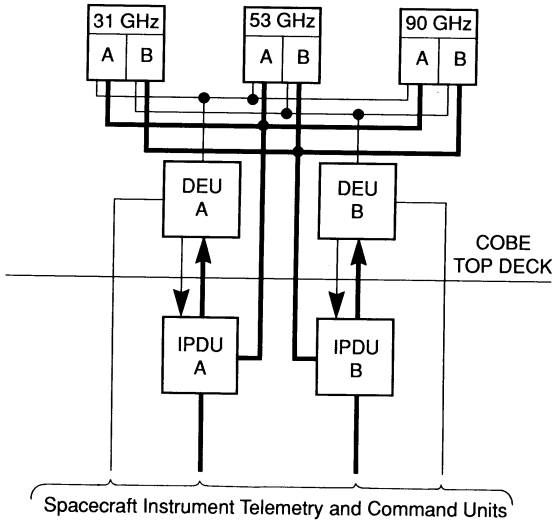

FIG. 3.—Schematic of the DMR experiment illustrating the interconnections of the instrument power distribution units (IPDUs), the data electronics units (DEUs), and the radiometer front ends labeled by frequency as 31, 53, and 90 GHz. The heavy solid lines indicate power and power-related signals handled by the IPDUs, and the other lines indicate other signals handled by the DEUs. The components above the line labeled "top deck" are physically located within the upper RF-shielded area inside the Earth/Sun shield.

are located symmetrically (every 120°) around the upper periphery of the dewar so that the horn antenna pairs of each radiometer view the sky symmetrically about the rotation axis of the spacecraft.

The two antennas for each receiver view fields which are 30° from the spacecraft spin axis and 180° apart in azimuth, i.e., 60° from one another. The spacecraft spin axis is nearly vertical, so the radiometers always view well away from the Earth. The receiver input is switched rapidly (at 100 Hz) between the two antennas. We measure and subtract the effect of asymmetry in the antennas by rotating the spacecraft at 0.8 rpm. Full sky coverage is obtained as the polar orbit slowly precesses with a 1 year cycle. The orbit and its precession effectively provide additional switching of the sky coverage with both 103 minute (14 orbits per day and 82 spins per orbit) and 6 month periods. It is important to ensure that nothing internal to the radiometer changes synchronously with any of these modulation periods.

b) *The Radiometers*

Each DMR unit contains two independent Dicke-switched radiometers, or channels, which operate at the same frequency and which share the same mechanical enclosure, thermal control systems, and some components such as redundant local oscillators and calibration noise sources. Figures 4–7 give schematic diagrams of the three DMRs, and Table 1 lists their important characteristics. The output of each channel is proportional to the temperature difference of the regions of sky viewed by its horn pair plus an additive constant. This additive constant, the instrumental offset, is measured by averaging over a spacecraft rotation. The data reduction strategy is to remove this offset and apply the calibration to obtain brightness temperature differences for pairs of sky pixels separated by 60°.

We have chosen an ambient temperature ($\sim$300 K) radiometer for the 31.5 GHz system and passively (radiatively)

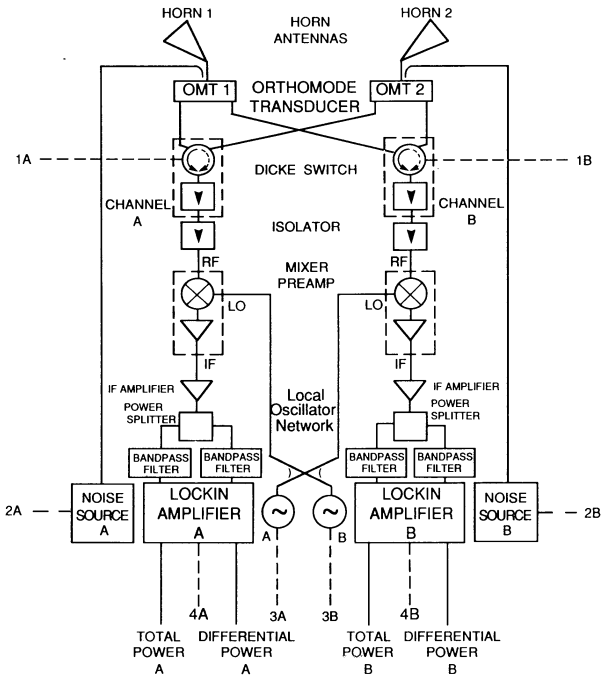

CONTROL FUNCTIONS (A/B AS INDICATED)
1. DICKE SWITCH MODE SELECTION: NORMAL PHASE, INVERSE PHASE, LOCK HORN 1, OR LOCK HORN 2
2. NOISE SOURCE ON/OFF
3. LOCAL OSCILLATOR ON/OFF
4. BANDWIDTH SELECTION: NARROW BAND OR WIDE BAND

FIG. 4.—A schematic diagram of the 31 GHz radiometer

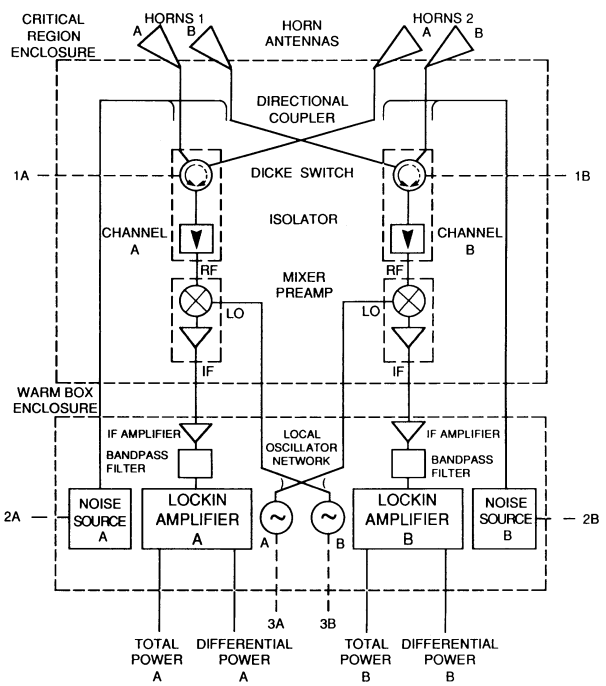

CONTROL FUNCTIONS (A/B AS INDICATED)
1. DICKE SWITCH MODE SELECTION: NORMAL PHASE, INVERSE PHASE, LOCK HORN 1, OR LOCK HORN 2
2. NOISE SOURCE ON/OFF
3. LOCAL OSCILLATOR ON/OFF

FIG. 5.—A schematic diagram of the 53 and 90 GHz radiometers

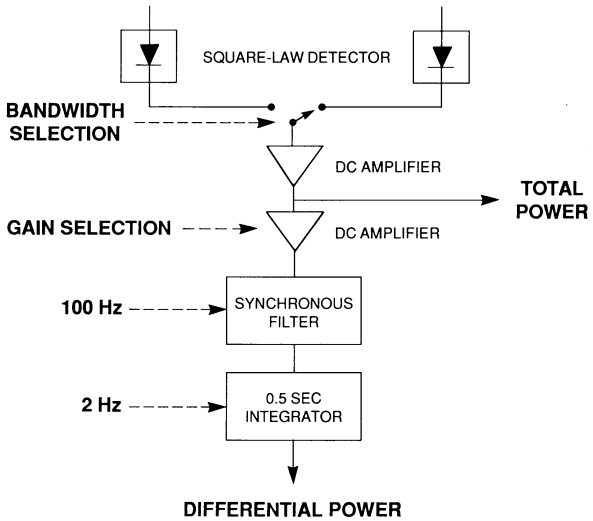

FIG. 6.—Schematic of the 31 GHz detection circuit (detector plus lock-in amplifier) design.

cooled radiometers (~140 K) for 53 and 90 GHz. A cooled radiometer, which can be made more sensitive than an ambient temperature radiometer, is more difficult to design, fabricate, and test. The 31.5 GHz system was kept as an ambient temperature radiometer as a result of trade-offs between the sensitivity advantages, and the extra complications associated with cooling and the resulting schedule delays and cost factors. Even with an ambient temperature 31 GHz radiometer, measurements of the CMB are expected to be limited by confusion from the galactic signal.

All three DMR units are functionally identical with the exceptions that the two 31 GHz channels share a common pair of horn antennas, and the bandwidths of these channels may be selected by command. The dimensions of the 31 GHz antennas

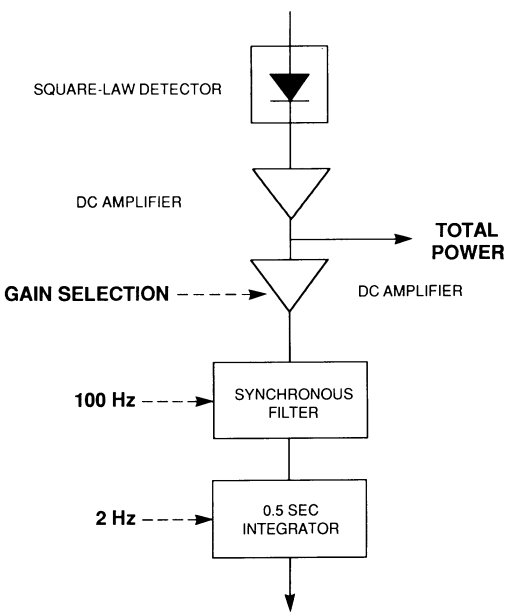

FIG. 7.—Schematic of the 53 and 90 GHz detection circuit (detector plus lock-in amplifier) design.

TABLE 1

RADIOMETER CHARACTERISTICS

CHARACTERISTIC	DMR CHANNEL					
	31		53		90	
	A	B	A	B	A	B
DT (mK $Hz^{-1/2}$)[a]:						
Normal mode	43	42	15.2	16.4	27.5	19.2
Alternate mode	66	39	...	...	...	...
IF bandpass (3 dB, MHz)[b]:						
Normal mode	44–557	44–569	1000–1827	1011–1833	1029–1823	1032–1900
Alternate mode	45–218	45–562	...	...	...	...
T_{sys} (K):						
Normal mode	391	380	205	206	302	240
Alternate mode	393	396	...	...	...	...
Dicke switch[c]:						
Model number	448-31	448-31	449-16	449-16	449D-17	449D-17
Serial number	PFU001	SPARE1	PFU002	PFU001	PFU001	PFU002
Frequency band (GHz)	30.9–32.1	30.9–32.1	51.2–54.8	51.2–54.8	88.2–91.6	88.2–91.6
Insertion loss (port 1, dB)	0.35	0.32	0.2	0.3	0.8	0.7
Insertion loss (port 2, dB)	0.31	0.30	0.3	0.4	0.7	0.6
Isolation (off port = 1, in dB)	29	31	25	22	20	28
Isolation (off port = 2, in dB)	29	31	25	24	21	27
Mixer/preamplifier assembly:						
Manufacturer	Hughes	Hughes	Hughes	Hughes	NASA/GSFC	NASA/GSFC
Model number	42311H-2000	42311H-2000	42314H-2000	42314H-2000	42316H-2000	42316H-2000
Serial number	8402	8403	8502	8504	101	103
Preamp manufacturer	Trontech	Trontech	Berkshire	Berkshire	GSFC	GSFC
Preamp type	Silicon	Silicon	GaAs FET	GaAs FET	HEMT	HEMT
Noise figure (dB)	3.1	3.0	2.0	2.1	2.5	2.4
Local oscillator:						
Manufacturer	Varian	Varian	Varian	Varian	Hughes	Hughes
Model number	VSA9010TC	VSA9010TC	VSE9020DK	VSE9020DK	47246H-1404S	47246H-1404S
Serial number	3150	3151	213	207	015	016
Frequency (GHz)[d]	31.505	31.502	53.014	53.006	89.993	89.963
Noise source:						
Manufacturer[e]	MSC	MSC	Hughes	Hughes	Hughes	Hughes
Model number	MC69134	MC69134	47143H-1000A	47143-1000A	47146H-1000A	47146H-1000A
Serial number	4600	4601	104	102	101	106
Type	Avalanche	Avalanche	Impatt	Impatt	Impatt	Impatt

[a] The sensitivity, DT (mk $Hz^{-1/2}$), is the rms noise for a 1 s integration period.
[b] The 31 GHz radiometer has a switchable second bandpass available, which is referred to here as the "alternate mode."
[c] All the Dicke switches are ferrite switchable latching circulators with output isolators, manufactured by Electromagnetic Sciences.
[d] The LO frequencies are for LOs A and B, respectively, although only a single LO runs both channels at any time.
[e] MSC = Microwave Semiconductor Corporation.

are sufficiently large to discourage the use of separate, identically pointed horn pairs as are used in the 53 and 90 GHz DMRs. Channels A and B of the 31 GHz radiometer receive opposite circular polarizations, whereas the 53 and 90 GHz channels receive a common linear polarization. The choice of narrow bandwidths for the 31 GHz radiometer (see Table 1) was included to allow for the possibility of interference which may appear in flight in the otherwise preferred broad bandwidth, which necessarily falls outside the narrow protected astronomy band at 31.4 GHz. An anomaly was found in the performance of the 31 GHz B-channel IF assembly late in the development program. Since the anomaly only occurred when the radiometer temperature was not in its nominal range, rather than disassembling and repairing the radiometer, we chose to replace the narrow bandwidth 31 GHz B-channel filter with a redundant wide-bandwidth filter.

A section of circular waveguide follows each horn antenna in the 31 GHz system and contains a matched dielectric (rexolite) plate to convert the incoming circular polarization into orthogonal linear waveguide modes (see Toral *et al.* 1989). This orthomode transducer directs the two orthogonal linear polarizations into separate receivers through matched rectangular waveguide sections (see Fig. 4). In-flight calibration signals are provided by noise diodes. Each orthomode transducer is fed by a separate noise source so that each channel receives two independent calibration signals. The signal from each noise source is injected through a directional coupler in a linear mode parallel to the dielectric plate, so that the noise source signal is approximately evenly divided between the two channels. If one noise source fails or becomes unreliable, the second noise source supplies the necessary calibration signal to both receivers. In the 53 and 90 GHz receivers (Fig. 5), the signal from each noise source is coupled into the waveguide sections which immediately follow the copointed horns of both channels, giving a noise source signal distribution which is functionally identical to that of the 31 GHz radiometer. The polarization of the 53 and 90 GHz receivers is such that the H-plane is parallel to the plane of the two horns of a given channel.

The output of the ferrite Dicke switch of each channel is alternated between the inputs from the two antennas. This is an essential step in the process of reducing systematic effects by reducing the effects of low-frequency gain fluctuations and $1/f$ noise in the radiometer amplifiers. Switching, however, introduces two new problems. First, when the switch to the antennas is pulsed to switch the receiver input from one antenna to the other, a transient signal occurs. Second, after switching, the antenna switch will generally have a different reflection coefficient or insertion loss. This is due to inherent small imperfections in the switch, and importantly, it may be modulated at the spacecraft spin rate by the changing aspect of the Earth's magnetic field. For this reason, the ferrite switch is magnetically shielded with as much high-μ Carpenter's steel (no. 49) as space permitted, and magnetic susceptibility measurements were made.

The output of the Dicke switch is sent through ferrite isolation to a mixer-preamplifier. The local oscillator (LO) signal is obtained from one of two Gunn diode oscillators which are coupled into the LO input ports of each receiver by a matched hybrid junction. Only one oscillator is turned on at any time, and the second provides redundancy in case of failure. The gains of the preamplifiers and postamplifiers are ~ 35 and ~ 40 dB, respectively, for all six channels.

The intermediate frequency (IF) outputs of the amplifiers are sent to individual lock-in amplifiers, as shown schematically in Figures 6 and 7. For each channel, this circuit consists of a square-law diode detector to convert the amplified IF power into a proportional voltage and an amplifier which is synchronized with the Dicke switch to detect the switch-modulated signal. The lock-in amplifier includes a circuit which integrates this switch-modulated signal for 0.5 s. This signal is subsequently sampled every 0.5 s by a digital converter in the DEU and multiplexed into the DMR data stream. The 31 GHz lock-in amplifier circuits (Fig. 6) are identical to those for the 53 and 90 GHz radiometers (Fig. 7) except for a bandpass selection feature. Each 31 GHz radiometer channel contains a power splitter which feeds two separate bandpass filters and detector diodes. A bandpass switch selects which postdetection voltage is sent to the lock-in amplifier. In addition, a gain selection command provides a factor of 75 to be switched to accommodate the differing scales of hot and cold load differences (~ 200 K) used in ground calibration and the noise sources (~ 2 K) which fly with the instrument.

c) Antennas

The antennas are wavelength-scaled corrugated horns similar to those used in previous anisotropy experiments (Smoot, Gorenstein, and Muller, 1977; Fixsen, Cheng, and Wilkinson 1983; Lubin *et al.* 1985) and described by Janssen *et al.* (1979). They were chosen for their low sidelobe response, low insertion loss, and compactness. Their nominal beamwidth is 7° full width at half-maximum power. Figure 8 shows sample measured beam patterns for the 31 and 53 GHz antennas. Details of the antennas and the measurements of their patterns are given by Toral *et al.* (1989).

These patterns combined with the attenuation of the Earth/Sun shield reduce extraneous emission to below the 0.1 mK level at all frequencies. The Earth/Sun shield was tested and found to meet its specification as a RF shield.

d) Thermal Control

The 31 GHz radiometer operates at 293 K. As indicated in Figure 5, the 53 and 90 GHz units are configured into two thermally isolated regions whose temperatures are separately controlled. Those components which generate significant amounts of heat such as amplifiers, local oscillators, and noise sources are segregated into an enclosure (warm box) which is regulated near 290 K. That portion of each radiometer (cold box) which is particularly vulnerable to temperature fluctua-

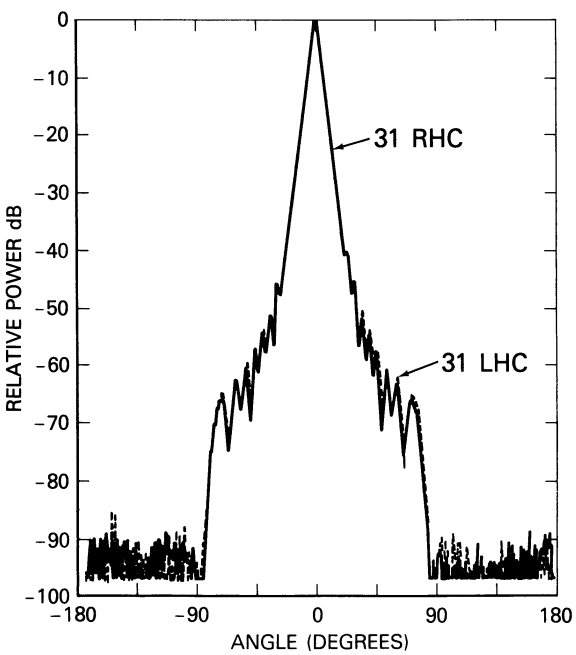

FIG. 8*a*

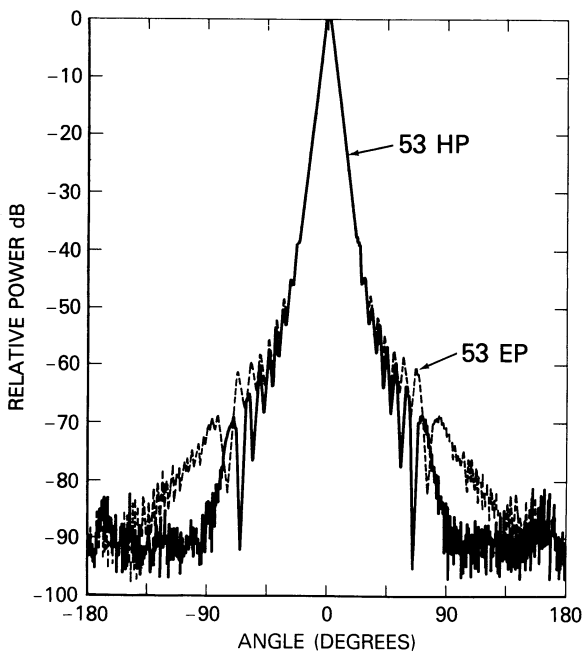

FIG. 8*b*

FIG. 8.—Sample beam patterns (from Toral *et al.* 1989) for (*a*) 31 GHz and (*b*) 53 GHz. (RHC indicates right-hand circular polarization, LHC indicates left-hand circular polarization, HP is H-plane polarization, and EP is E-plane polarization.)

tions is separately enclosed and regulated at 139 K. The temperatures of both enclosures are actively controlled to ensure long-term radiometer stability. In the cases of the 53 and 90 GHz radiometers, where low temperatures are used to maximize sensitivity, the cold box enclosures are radiatively cooled to as low a temperature as practical. A high thermal impedance is required on the mechanical and waveguide components between the warm box and cold box regions. The passive cooling of the 53 and 90 GHz DMRs is described in greater detail by Mengers, Kroliczek, and Harrison (1985).

The instrument has several proportional DC thermal-control systems which regulate and monitor temperatures, with particular attention to crucial components. The relatively constant thermal environment in space enhances the stability of the instrument. A schematic view of the locations and types of temperature sensors is shown in Figure 9.

Tests performed on the individual instruments and on the fully assembled spacecraft, done in vacuum, verified the proper thermal operation of the instrument.

e) Instrument State Commands

The radiometer states may be individually set by external commands as indicated in Figures 4–7. In addition to the 31 GHz IF bandpass selection, commands can be given to switch the gain, select the mode of the Dicke switches, switch local oscillators, and activate noise sources. The local oscillators may be individually commanded to turn on or off, and four modes may be selected for the Dicke switches: (1) normal switching at 100 Hz, (2) inverted (i.e. 180° phase shifted) switching at 100 Hz, (3) lock to horn 1, and (4) lock to horn 2. In routine flight operation, the preferred local oscillator is left on at all times, the Dicke switch operates in the normal switching mode, the gain is in the "high-gain" mode, and the noise sources are turned on periodically for calibration. The remaining states will be available for diagnostic purposes, if necessary, and have been used extensively in preflight calibrations.

f) Telemetry

The output of the 0.5 s integrator of the lock-in amplifier circuit is digitized with a 12 bit analog-to-digital converter. These data, along with instrument housekeeping data, are telemetered with the other *COBE* satellite signals at 4096 bits per second (in 512 eight-bit words) with a minor frame every 0.25 s and a major frame every 32 s (every 128 minor frames). There are 64 data samples per major frame of DMR science data for each frequency, with the 31 and 53 GHz data on even minor frames and the 90 GHz data on odd minor frames. The DEU housekeeping data are sampled four times per major frame (every 8 s in 12 bit words) and the IPDUs are sampled once per major frame (every 32 s in eight-bit words). The housekeeping data include temperatures, voltages, currents, and state monitoring. The total DMR data rate is ~ 1 Gbyte per year.

g) Mass and Power Consumption

The DMR box masses were measured individually, and the results are given in Table 2. A minimum box thickness of 3/32 of an inch was required to provide protection from the expected nuclear radiation environment. In addition to the individual box masses in Table 2, there are several harnesses interconnecting the boxes which have significant mass.

The DMR experiment uses 123 watts of about 750 watts of available spacecraft power provided by solar panels. This includes all three radiometers, their instrument power distribution units, and their digital electronics units, as shown in Table 3. As can be seen, the total DMR power usage is approximately equally split between power used for heaters and power used for the electronics. Except for small variations in the heater power required during the course of the mission, the total instrument power requirements will be nearly constant.

IV. ENGINEERING TESTS AND CALIBRATION

a) Tests and Test Equipment

The engineering tests and calibrations were aimed at assuring that the instruments function properly, with high stability, high sensitivity, low susceptibility to potential interfering effects, and accurate calibration.

Many component level tests and measurements were carried out, such as LO frequency and stability and IF bandpass shape measurements. The following tests and measurements were made of the fully assembled instrument system: verification that all command states give expected output; measurement of the system noise figures; measurement that noise levels average down as the square root of time; measurement of the system linearity; noise source temperatures and stability; measurement of the calibration (Kelvin per telemetry data unit); effect of small temperature deviations on the calibration and operation; gain ratios between high- and low-gain radiometer settings; radiometric offset when looking at equal temperature targets; susceptibility to externally applied magnetic fields; susceptibility to artificially exaggerated DC bus voltage fluctuations.

All these tests provided acceptable results except for the magnetic susceptibility. The worst case is 0.6 mK G^{-1} along the spin axis of the 53 GHz A-channel. Some magnetic effect removal will be necessary in the data reduction software after a year of data averaging. This should not be a major concern since the effects are small, given that both the Earth's field and the torquer bar fields are relatively well known and the susceptibility of the instrument is measured.

Most of the instrument-level tests used a thermal-vacuum chamber with a rotating cold target and a warm calibration target. The chamber consisted of an instrument shroud through which LN_2 circulated to keep the instrument at the desired cooled temperature, an LN_2 cooled dish with micro-

TABLE 2

DMR MASS SUMMARY

	RADIOMETERS			DEUs		IPDUs	
MASS	31 GHz	53 GHz	90 GHz	A	B	A	B
English (lb)[a]	73.0	83.0	79.0	11.3	11.3	40.5	40.5
Metric (kg)	33.1	37.6	35.8	5.12	5.12	18.4	18.4

NOTE.—Total DMR mass = 153.6 kg (338.6 lb).

[a] Actual weights ±0.1 lb.

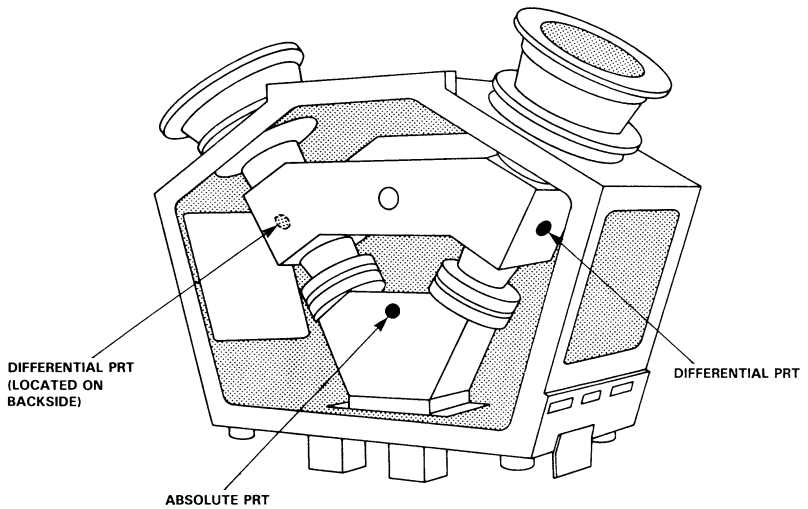

FIG. 9*a*

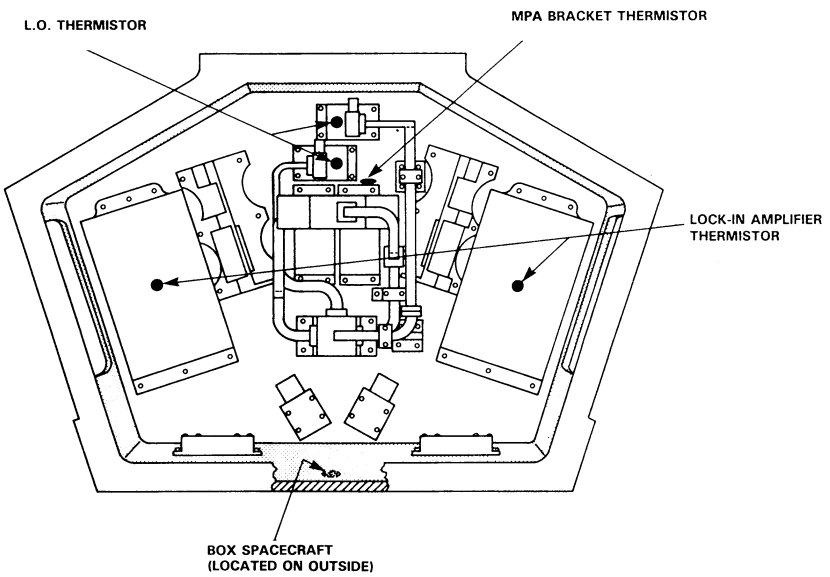

FIG. 9*b*

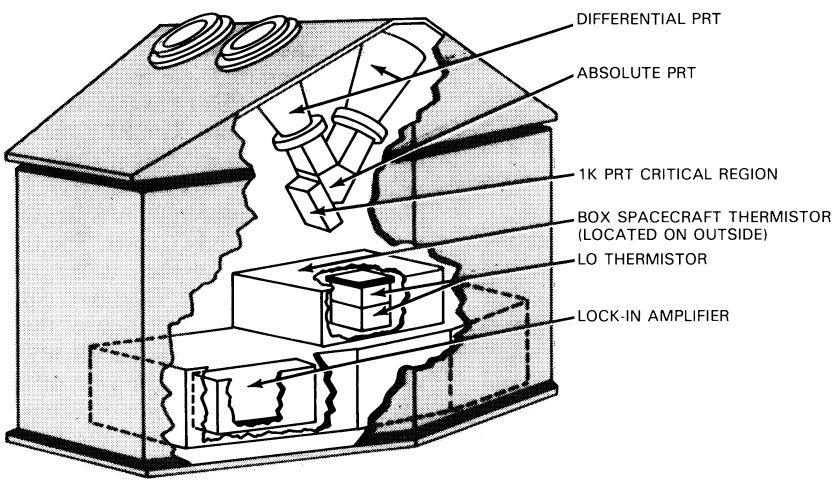

FIG. 9*c*

FIG. 9.—Schematic view of the locations of temperature sensors on the (*a*), (*b*) 31 GHz radiometer, and (*c*) on the 53 and 90 GHz radiometers. The sensors are either thermistors or platinum resistance thermometers (PRTs), as indicated.

TABLE 3

DMR POWER CONSUMPTION

POWER USE	31	53	90	DEU	IPDU	Total
Channel A	8.22	3.13	10.14	4.27	18.26	36.40
Channel B	3.18	8.42	3.57	4.22	15.25	28.60
Total (instrument)	11.40	12.55	13.71	8.49	33.51	65.00
Heater Bus A (case, warm box)	12.56	9.93	9.26	5.40	...	37.12
Heater Bus B (critical regions)	9.21	2.23	2.53	6.40	...	20.37
Total (heaters)	21.77	12.16	11.76	11.80	...	57.49
Totals	33.17	24.71	25.47	20.29	33.51	122.49

NOTE.—All numbers in watts.

wave target material to serve as a "cold" load, a "warm" load microwave target material which is motor driven to fill one or the other of the horns' beam pattern, vacuum gauges, temperature sensors, and a vacuum pump. The "cold" target was rapidly spun synchronously with the analog data integration rate to assure that the radiometer sees equal temperatures in each beam. A "spacecraft interface simulator" provided the instrument with a power, control, and telemetry interface which imitate the spacecraft.

b) Radiometer Characteristics

Table 1 shows the important radiometer characteristics. The measured sensitivities of the radiometers were obtained by examining the rms noise when using targets of known temperature, and they are approximately consistent with the standard *Y*-factor technique (see, for example, Evans and McLeish 1977). The radiometer gains were adjusted to give approximately 2 mK per telemetry data unit in the high-gain mode, and approximately 150 mK per data unit in the low-gain mode. The sensitivity of the radiometers to gain modulated systematic effects has the functional form of the error times the instrument radiometric imbalance, or offset. The radiometer offsets were made adjustable by the use of small screws with absorbing material at the end which can penetrate the waveguide. By choosing combinations of components to minimize imbalance, the radiometric offsets for all six channels were below 2 K. Final adjustment of the screws was done at the time of final instrument-level testing, further reducing all the offsets to below 0.2 K, before the instrument was integrated with the spacecraft. Shortly before the spacecraft was to be shipped to the launch site, contamination was found near the polarizer deep inside a 31 GHz horn. The contaminant was removed, and the offset on the 31 GHz A-channel was measured to change to 0.7 K, but no further offset screw adjustment was made.

c) Calibration

On-board noise sources are used to determine the stability of the radiometer calibration in flight. The on-board solid-state diode noise sources were calibrated in ground testing against known hot and cold loads. The stability of the noise source calibration was checked by measuring over a period of time. The noise sources are used to transfer the laboratory hot and cold load calibration to operation in space. The noise sources are turned on and off in orbit, by command, approximately every 2 hours. A check on the stability of the noise sources can be provided by comparing with observations of the Moon, which is visible roughly 2 weeks per month. The detailed calibration results will be presented in a future paper.

d) Expected Performance

In 1 year of observation, the 53 and 90 GHz instruments are capable of mapping the sky to an rms sensitivity of 0.1 mK per 7° field of view. This translates to a per pixel sensitivity of $\Delta T/T_{\rm CMB} = 4 \times 10^{-5}$ (1 σ) and a dipole sensitivity of 5×10^{-6} (1 σ) in 1 year. Further sensitivity improvement may be achieved by combining the results of the six nearly independent radiometer channels. The instrument was designed to operate for one full year, and current plans are to operate for 2 years. The scientific significance of such sensitivities for some aspects of cosmology is discussed by Bennett and Smoot (1989).

e) Space Qualification Testing

In the early instrument development stage, mechanical qualification structures were built and tested. These tests included responses to static loads, shocks, random vibrations, and sine wave excitations. Detailed computer models of the structures were also developed, and test data were fed back into the models for a more complete understanding of the structures. Structural changes were iterated until acceptable results were attained, and then protoflight structures were built for the microwave radiometers.

The microwave radiometers were vibrated to 1.25 times higher levels than expected during the Delta rocket launch. The radiometers were vibrated a second time during a full spacecraft vibration test, also to 1.25 times greater amplitude than expected. The functionality and calibration of the radiometers were intact after each vibration test.

Several space qualification tests were carried out on the integrated spacecraft. These included external RFI compatibility tests, self-compatibility tests, vibration, acoustics, shock, and thermal performance. The RFI tests were performed with the spacecraft in a large RF-tight room with RFI levels generated as high as 5 V m^{-1} from 1–12 GHz. The mechanical tests were done with the spacecraft in a large vibration facility at the Goddard Space Flight Center. The thermal tests were done in a large vacuum chamber, called the Solar Environmental Simulator, also at the Goddard Space Flight Center. This chamber allowed a simulation of the temperature transitions which the spacecraft undergoes in attaining its nominal orbital thermal state, as well as its operation in that nominal state, and the effects of the eclipse season. These simulations are important not just for the instruments, but for the complicated attitude control system, power subsystem, and command and data handling subsystem as well.

Each of the concerns revealed by these tests were resolved either by system modifications or by a decision that no action

was required. In addition to all the special qualification tests outlined above, the instruments were operated in various environmental conditions to assure their proper operation.

V. SUMMARY

Differential Microwave Radiometers (DMRs) have been designed, built, and tested at 31.5, 53, and 90 GHz to map the large-scale anisotropy of the cosmic microwave background radiation. Particular attention has been paid not only to the sensitivity of the radiometers, but also to their stability and to their ability to reject systematic effects which have limited previous measurements.

The DMR experiment is flying aboard the *Cosmic Background Explorer* (*COBE*) satellite with the FIRAS and DIRBE experiments. These experiments will produce a major step forward in observational cosmology.

We are grateful to the NASA *COBE* Project for their support of this work. We wish to thank the many people at the NASA Goddard Space Flight Center who designed, built, and tested the microwave radiometers. In particular, we thank R. Aleman, D. Amason, M. Bukowski, C. Collins, J. Cottrell, M. Donohoe, I. Errera, B. Gabbert, J. Gibson, G. Gochar, F. Gross, P. Haney, R. Hanold, H. Johnson, F. Jones, F. Kirchman, B. Klein, C. Kotecki, A. Lacks, J. Lecha, R. Martin, R. Mattson, D. McCarthy, D. McDermont, G. Miller, J. Muller, D. Nace, S. Petro, S. Rapp, E. Seader, S. Servin-Leete, C. Witebsky, B. Wittig, J. Wolfgang, E. Young, and P. Young. We are also grateful to Tony Kerr of the National Radio Astronomy Observatory for his help in producing the 90 GHz mixer-preamplifiers.

REFERENCES

Alpher, R. A., and Herman, R. 1948, *Nature*, **162**, 774.
———. 1949, *Phys. Rev.*, **75**, 1089.
———. 1950, *Rev. Mod. Phys.*, **22**, 153.
———. 1975, *Proc. Am. Philos. Soc.*, **119**, 235.
Batakis, N., and Cohen, J. M. 1975, *Phys. Rev. D*, **12**, 1544.
Bennett, C. L., and Smoot, G. F. 1989, in *Relativistic Gravitational Experiments in Space*, ed. R. W. Hellings (NASA Conf. Pub. 3046), p. 114.
Boughn, S. P., Cheng, E. S., Cottingham, D. A., and Fixsen, D. J. 1990, *Rev. Sci. Instr.*, **61**, 158.
Bromberg, B. W., and Croft, J. 1985, in *Proc. Annual Rocky Mountain Guidance and Control Conf. of the American Aeronautical Society*, ed. R. D. Culp, E. J. Bauman, and C. A. Cullian (San Diego: Am. Aeronautical Soc.), p. 217.
Burke, W. L. 1975, *Ap. J.*, **196**, 329.
Cheng, E. S., Saulson, P. R., Wilkinson, D. T., and Corey, B. E. 1979, *Ap. J. (Letters)*, **232**, L139.
Collins, C. B., and Hawking, S. W. 1973, *M.N.R.A.S.*, **162**, 307.
Dicke, R. H., Peebles, P. J. E., Roll, P. G., and Wilkinson, D. T. 1965, *Ap. J.*, **142**, 414.
Evans, G., and McLeish, C. W. 1977, *RF Radiometer Handbook* (Dedham, MA: Artech House).
Fixsen, D. J., Cheng, E. S., and Wilkinson, D. T. 1983, *Phys. Rev.*, **50**, 620.
Gamov, G. 1948*a*, *Phys. Rev.*, **74**, 505.
———. 1948*b*, *Nature*, **162**, 680.
Gödel, K. 1949, *Rev. Mod. Phys.*, **21**, 447.
Grishchuk, L. P., and Zel'dovich, Ya. B. 1978, *Soviet Astr.*, **22**, 125.
Hawking, S. W. 1969, *M.N.R.A.S.*, **142**, 129.
Janssen, M. A., Bednarczyk, S. M., Gulkis, S., Marlin, H. W., and Smoot, G. F. 1979, *IEEE Trans. Ant. Prop.*, **AP-27**, 551.
Klypin, A. A., Sazhin, M. V., Strukov, I. A., and Skulachev, D. P. 1987, *Soviet Astr. Letters*, **13**, 104.
Lubin, P., Villela, T., Epstein, G., and Smoot, G. 1985, *Ap. J. (Letters)*, **298**, L1.
Mather, J. C. 1982, *Opt. Engineering*, **21**, 769.
Mather, J., and Kelsall, T. 1980, *Phys. Scripta*, **21**, 671.
Mengers, D. R., Kroliczek, E. J., and Harrison, R. E. 1985, in *Proc. AIAA 20th Thermophysics Conf.*, (New York: American Institute of Aeronautics and Astronautics),
Partridge, R. B. 1987, in *IAU Symposium 124, Observational Cosmology*, ed. A. Hewitt, G. Burbidge, and L. Z. Fang (Dordrecht: Reidel), p. 31.
Penzias, A. A., and Wilson, R. W. 1965, *Ap. J.*, **142**, 419.
Sachs, R. K., and Wolfe, A. M. 1967, *Ap. J.*, **147**, 73.
Smoot, G. F., Gorenstein, M. V., and Muller, R. A. 1977, *Phys. Rev. Letters*, **39**, 898.
Strukov, I. A., and Skulachev, D. P. 1984, *Soviet Astr. Letters*, **10**, 1.
———. 1988, *Ap. Space Phys. Rev.*, **6**, 145.
Strukov, I. A., Skulachev, D. P., Boyarskii, M. N., and Tkachev, A. N. 1988, *Soviet Astr. Letters*, **13**, 65.
Thorne, K. S. 1967, *Ap. J.*, **148**, 51.
Toral, M. A., Ratliff, R. B., Lecha, M. C., Maruschak, J. G., Bennett, C. L., and Smoot, G. F. 1989, *IEEE Trans. Ant. Prop.*, **37**, 171.
Vilenkin, A. 1985, *Phys. Rept.*, **121**, 263.
Wilkinson, D. T. 1986, *Science*, **232**, 1517.
———. 1987, in *IAU Symposium 130, Large Scale Structures of the Universe*, ed. J. Audouze, M. Pelletan, and A. Szalay (Dordrecht: Kluwer), p. 7.

CHARLES BACKUS, CHARLES BENNETT, NANCY BOGGESS, ED CHENG, MICHAEL G. HAUSER, TOM KELSALL, JOHN MATHER, HARVEY MOSELEY, RICHARD SHAFER, and ROBERT SILVERBERG: Laboratory for Astronomy and Solar Physics, Code 680, NASA/Goddard Space Flight Center, Greenbelt, MD 20771

JOHN CHITWOOD, LARRY HILLIARD, MARIA LECHA, JOHN MARUSCHAK, RICHARD MILLS, ROBERT PATSCHKE, ROGER RATLIFF, and CATHY RICHARDS: Instrument Division, Code 720, NASA/Goddard Space Flight Center, Greenbelt, MD 20771

S. GULKIS and M. JANSSEN: Jet Propulsion Laboratory, 4800 Oak Grove Drive, Pasadena, CA 91109

P. LUBIN: Physics Department, University of California, Santa Barbara, CA 93106

T. MURDOCK: Technology Department, General Research Corporation, 5 Cherry Hill Drive, Danvers, MA 01923

G. SMOOT: Lawrence Berkeley Laboratory, MS 50-232, University of California, Berkeley, CA 94720

R. WEBER: EOS Project, Code 415, NASA/Goddard Space Flight Center, Greenbelt, MD 20771

R. WEISS and S. MEYER: Massachusetts Institute of Technology, Room 20-F006, Cambridge, MA 02139

D. WILKINSON: Department of Physics, Jadwin Hall, Princeton University, Princeton, NJ 08540

E. WRIGHT: Department of Astronomy, University of California, Los Angeles, Los Angeles, CA 90024